Science Press

ARTICLE

Preparation and Corrosion Resistance of Laser-Cladded Cu-Based Alloy Coatings on Q235 Steel

Kong Yao,   Liu Zongde,   Li Bin

Key Laboratory of Power Station Energy Transfer Conversion and System, Ministry of Education, North China Electric Power University, Beijing 102206, China

Abstract: Copper-based coatings were prepared on the surface of Q235 steel by fiber laser under different powers. Microstructure, phase composition, corrosion resistance of the coatings were revealed by scanning electron microscopy (SEM) equipped with energy dispersive spectrometry (EDS), X-ray diffraction (XRD) and electrochemical workstation, respectively. Results show that the coatings are well bonded to the substrate. The coating microstructure consists of cellular, coarse dendrites, fine dendrites and columnar grain structure from the bottom to the top. The coatings mainly contain two phases including Cu(Ni,Fe) and Ni(Cr,Mo,Fe) solid solution. The coating with two layers prepared under 2000 W exhibits optimal corrosion resistance due to its highest corrosion potential and lowest corrosion current density.

Key words: copper-based coating; laser cladding; microstructure; corrosion resistance

According to recent researches, the loss caused by steel corrosion in China accounts for about 10% of the total steel output[1]. The mechanical parts exposed to corrosive environment, such as ships, pipelines of oil and gas, and boiler tubes in power plants, are necessary to have good corrosion resistance for prolonging their service life. Nowadays, some literatures have investigated Cu-based alloy and indicated its satisfying behavior in the seawater corrosion resistance and marine organism fouling protection. Copper (Cu) and its alloys possess high electrical, thermal conductivity, and better corrosion resistance[2]. Most Cu alloys have better corrosion resistance under atmospheric and marine environment because of its high electrode potential[3,4]. Adding some metal elements to the Cu matrix is an effective way to increase the corrosion resistance and to expand application of Cu coatings. Ni, Cr, W, Mo, B and Si elements have already been adopted as alloying elements for Cu coatings to improve the corrosion resistance.

Preparation method is also an important part beyond raw material to improve corrosion resistance of mechanical parts surface. In order to enhance corrosion resistance with low cost, surface coatings are widely fabricated by electroplating, thermal spraying, physical vapor deposition (PVD), etc. Surface coatings can combine the properties of both the reinforcement material and the substrate. However, the coatings fabricated by these conventional methods above cannot be strongly bonded to the substrate. Laser cladding is an advanced surface modification technique to improve the surface hardness, anti-corrosion properties and wear resistance, which has gained great popularity in the past few decades. Compared with other conventional surface treatment techniques, such as thermal spraying and plasma transferred arc welding, laser cladding has some unique features such as rapid melting and solidification cycle at localized region, low heat distortion to the substrate and formation of strong metallurgical bonding between the coating and the substrate[5,6]. Laser cladding has been widely investigated in terms of microstructure evolution, phase change, corrosion resistance, and optimum processing parameters[7-11].

Laser cladding with Cu-based alloys is a feasible way to improve the corrosion resistance of mechanical parts. Zhang[12] prepared corrosion-resistant coatings of Ni-Cr-Cu alloy, which possess excellent corrosion resistance in marine atmosphere. They found that Ni can improve the corrosion potential of

substrate and increase corrosion resistance under high Cl⁻ concentrations, and Cr is gathered to form the compact film. The combination of Cr, Ni and Cu provides a better protective coating for substrate against corrosion. Liu[13] studied the effect of adding Mo on corrosion resistance of Cu-based bulk amorphous alloy. They found that the corrosion resistance of Cu-base bulk amorphous alloy is obviously improved after adding Mo. Oldfield[14] studied the corrosion resistance of nickel aluminum bronze, stainless steel and high nickel cast iron applied to pipe system. The results showed that nickel aluminum bronze has better stress corrosion and fatigue corrosion resistance than other alloys. Wang[15] studied the corrosion resistance of Cu coating on magnesium alloy prepared by electrolytic deposition. It was found that the corrosion resistance of magnesium alloy is improved obviously. The tidy and dense Cu coating provides protection for the magnesium substrate continuously up to 60 h.

In this work, Cu-based coatings were prepared on Q235 steel by laser cladding under different laser powers. In order to understand the effect of laser power and number of cladding layers on element dilution and corrosion resistance, microstructure, phase constitution and element dilution of coatings were investigated by XRD, SEM and EDS. The corrosion resistance was studied by electrochemical techniques.

1　Experiment

Laser cladding system used in this work consists of four parts: the fiber laser as the energy source, the three-axis computer numerical controlled cladding workbench, an argon shielding gas system and the flowing water cooling water system. The parameters of laser cladding process are shown in Table 1.

In the present investigation, Q235 steel with dimensions of 150 mm×150 mm×10 mm was used as substrate material. The substrate was ground and subsequently cleaned with alcohol prior to the cladding process to remove surface oxide and enhance adhesion to preplaced alloy powder. The chemical composition of Q235 steel substrate and Cu-based alloy is listed in Table 2 and Table 3, respectively. The particle diameter of the Cu-based alloy powders is 45~109 μm and the powders were dried at 100 °C for 6 h in the DH-101 Elector-thermostatic blast oven. Argon was used as the shielding gas to provide an oxide free atmosphere. The Cu-based alloy powders were preplaced onto the surface of substrate and the thickness was controlled to 1 mm. Multitrack cladding was used to prepare the first layer with a desired thickness of 700 μm, and then the first layers of S1, S2, S3 were polished and

degreased. The process of powder pre-placement and laser treatment was repeated for cladding the second layer. After laser cladding, all of the as-prepared samples with dimensions of 10 mm×10 mm×10 mm were cut perpendicular to the surface by wire cut machining. The surface and cross-section of samples were wet ground by abrasive SiC papers from 400# up to 2000# grit and then polished with diamond paste. Finally, the samples were ultrasonically cleaned in acetone, ethanol and deionized water. The cross-section of the samples was etched by aqua regia for 15 s for microstructure observation via scanning electron microscope (SEM) equipped with an energy dispersive spectrometer (EDS). The samples for electrochemical test were sealed with epoxy resin, leaving a working electrode area of 10 mm×10 mm. Then electrode surface was wet ground by SiC abrasive paper from 400# to 2000# grit, and then polished and ultrasonically cleaned in acetone, ethanol and deionized water. Finally, all the coatings were cleaned again, dried and packaged for further testing and analysis.

2　Results and Discussion

2.1　X-ray diffraction analysis

Phase compositions of four coatings are identified from the XRD patterns, as shown in Fig.1. It can be observed that all coatings have almost the same pattern. The number of cladding layers and different laser powers have nearly no effect on the products in coatings because of the same phase composition and intensity, which is consistent with the relevant microstructure. The phase mainly contains Cu(Ni,Fe) solid solution because of the infinite mutual solubility between Cu and Ni. Furthermore, the low intensity peak corresponds to precipitated phase Ni(Cr, Mo, Fe), and the lowest diffraction peaks of $MoNi_4$ and $Mo_{12}Fe_{22}C_{10}$ are detected. Fe can easily diffuse from substrate to the coatings under the high energy input during the cladding process, which makes it react with the elements in Cu-based alloy. Based on the laser cladding process of heating-cooling-featured, the formation of Cu(Ni,Fe) solid solution releases a large extra amount of heat, combined with the heat released form the melting pool, which provides the energy to form the intermetallic compounds like $MoNi_4$ and $Mo_{12}Fe_{22}C_{10}$. The intermetallic compound can increase the liquidity of the melting pool, which can help decrease the tendency of initiation and propagation of micro-crack in the coatings. Furthermore, the presence of intermetallic compounds functions well in improving the average hardness of the coatings.

2.2　Microstructure and elements analysis

The SEM images of whole cross-section morphology of

Table 1　Laser cladding process parameters

Sample	Laser output power/W	Scan speed/mm·s⁻¹	Beam diameter/mm	Overlap width/mm	Cladding layer number
S1	1600	3.2	2.8	1.5	2
S2	1800	3.2	2.8	1.5	2
S3	2000	3.2	2.8	1.5	2
S4	1800	3.2	2.8	1.5	1

Table 2   Compositions of Q235 steel substrate (wt%)

Si	Mn	S	P	C	Fe
0.37	0.08	0.04	0.04	0.16	Bal.

Table 3   Compositions of Cu-based alloy (wt%)

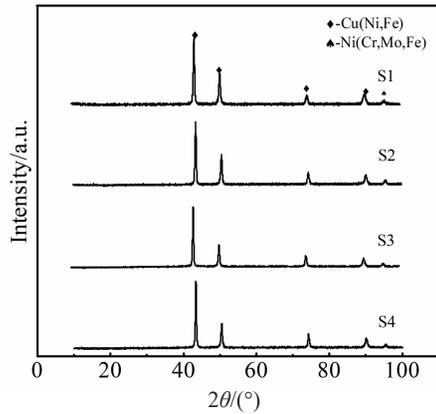| Ni	Mo	Cr	Si	Cu
24.83	2	12.08	0.04	Bal.

Fig.1   XRD patterns of coatings S1, S2, S3 and S4

coatings S1, S2, S3 at low magnification are shown in Fig.2. Coatings are well bonded to the substrate, and free from obvious cracks. Interfaces between the coatings and substrate are not flat and not straight because of overlapped concave profile and Gaussian energy distribution of the laser beam. It also brings about the inconsistent depth of molten pool but will not affect the main coating properties. In the process of laser cladding, powders absorb laser energy much more efficiently than the substrate does as powders are preplaced on substrate. Then powders together with substrate are melted upon absorption of laser energy. According to the figures above, coatings mainly contain two phases. Energy dispersive X-ray spectra show a light gray structure based on Cu-riched phase and the other is Fe-riched phase in dark gray with circle shape.

The detail of cross-section microstructures corresponding to coatings from bottom to top surface is given in Fig.3. In laser cladding process, the Cu-based alloy and the substrate solidify rapidly when the laser beam moves away from the laser-molten pool. The morphology mainly depends on the temperature gradient (G) and solidification rate (R) and the G/R. The G/R greatly affects microstructure of the coatings. In the middle of the coating, high temperature gradient and low solidification rate lead to the growth of dendritic grain. The cold substrate creates a high cooling rate at the beginning of the cladding, which produces the fine cell in the bottom of the coating. But at the bond zone of the first and second cladding layer, the temperature gradient is not very high because the first layer we fabricated has a little heat loss, and the grains are more irregularly dendritic. Accompanying the continuous argon gas flow, the cooling rate is greatly increased on the top surface of the coatings, which produces the uniform sphere eutectic.

A minimum dilution is necessary to guarantee a good
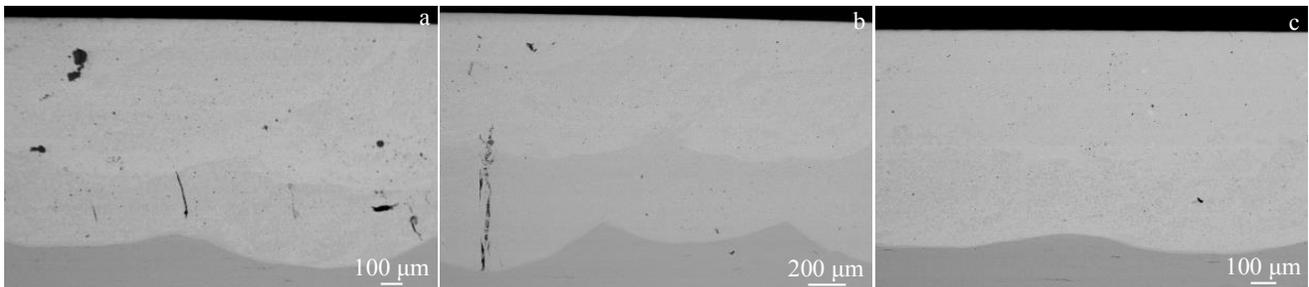

Fig.2   SEM images of cross-section morphology of coatings S1 (a), S2 (b) and S3 (c) at low magnification
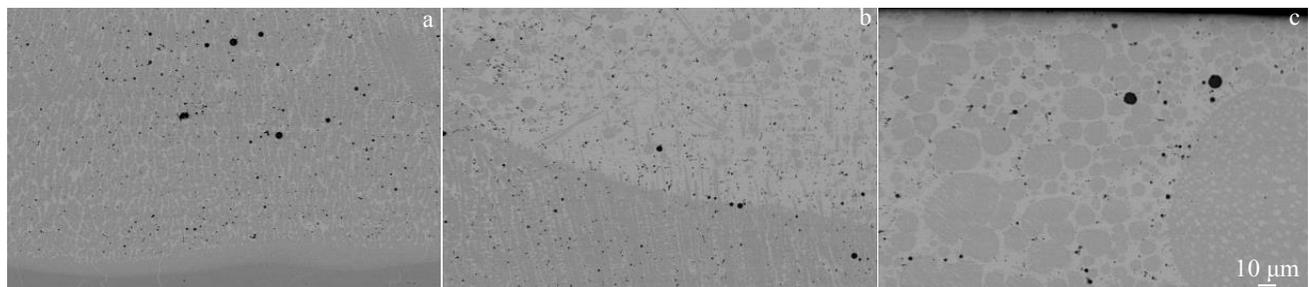

Fig.3   SEM images of cross-section microstructures of bottom (a), middle (b) and top (c) for coating S1

metallurgical bonding between coating and substrate, so an excessive dilution is undesirable, which may change the chemical composition and properties of the coating. In this work, the content of elements in selected area from the coating surface to the substrate was measured by SEM equipped with EDS. The diffusion curves of five elements (Cr, Fe, Ni, Cu, Mo) in the coatings are shown in Fig. 4. The content of Fe rapidly decreases from the substrate to coating surface. In coatings S1, S2 and S3, the content of Fe is around 17wt%, 40wt% and 47wt%, at which the distances to substrate are 400~600, 200~400 and 200~600 μm, respectively. On the contrary, the content of Cu is around 70wt%, 45wt%, 35wt%, at which the distances to substrate are 400~600, 200~400 and 200~600 μm, respectively. The content of other three elements (Cr, Ni, Mo) has a very small fluctuation, which means that all of them are distributed uniformly. The content of Fe and Cu significantly fluctuate in the coatings accompanied with the increase of laser power. It can be concluded that the most effective way to decrease the diffusion of Fe and Cu is cladding twice at power of 1600 W. By increasing the laser power and keeping the laser scanning speed constant, the heat input increases. It seems that at high laser powers, both the molten turbulence and the molten pool depth increase. Thus, the gas absorption probability increases. There are some defects observed in coatings S1 and S2. This is because the gas does not have enough time to escape from the porosity during the solidification process with the rapid solidification rate, especially in such a high heat input. The first layer is found much thinner than the second layer. This is because the first layer is remelted when fabricating the second layer,

resulting in the drastic fluctuation of content of Fe and Cu. In the second layer cladding process, laser provides enough energy for Fe to diffuse from the first layer up to the second layer. The higher the laser power, the higher the Fe content in the coatings.

From bottom to top surface of the coating, the Fe content in the coating S4 is near 35% with little fluctuation, which is much higher than that in the other three coatings. Two cladding layers can effectively decrease the dilution by preventing Fe diffusion, especially at laser power 1800 W.

2.3 Electrochemical measurements

Potentiodynamic polarization curves for coatings S1, S2, S3, S4 in 3.5% NaCl solution are plotted in Fig. 5 and they show similar trend. The vertical coordinate is the corrosion current density of the working electrode surface. The horizontal coordinate is the potential of the electrode with a platinum electrode. The corrosion potential (E_{corr}) and corrosion current density (I_{corr}) values were extracted from the plots by Tafel extrapolation method.

The corrosion potential (E_{corr}) and evaluation of the corrosion current density (I_{corr}) of four coatings are shown in Table 4. Coating S3 displays the most positive corrosion potential of about -226 mV and the lowest corrosion current density compared to other coatings. Coating S2 has the lowest corrosion potential of about -438 mV and the highest corrosion current density. Coating S4 has the lower corrosion current density of about $1.321×10^{-6}$ A/cm². The corrosion current density of coating S1 is about $3.517×10^{-6}$ A/cm². The dense and tiny coatings are formed to prevent the coatings from corrosion.
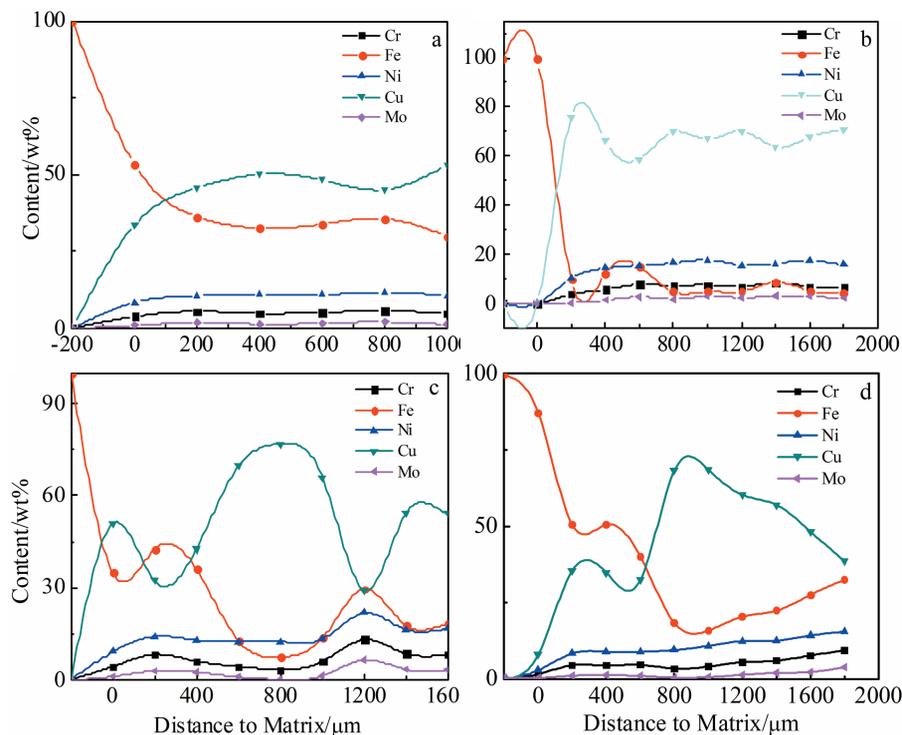

Fig.4　Element content change curves with the distance to matrix for coatings S1 (a), S2 (b), S3 (c), and S4 (d)
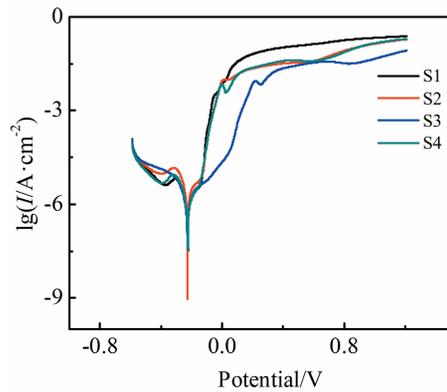
Fig.5　Polarization curves of coatings S1, S2, S3 and S4

Table 4　Electrochemical parameters of coatings S1, S2, S3 and S4

Coating	E_{corr}/mV	I_{cor}/$\times 10^{-6}$ A·cm^{-2}
S1	-237	3.517
S2	-438	3.566
S3	-226	1.074
S4	-236	1.321

The corrosion potential is the basis for evaluating corrosion resistance of the material. The higher the corrosion potential, the lower the possibility of corrosion. The corrosion rate depends on the corrosion current density once corrosion happens. It can be concluded from Table 4 that coating S3 will be more difficult to corrode than other three coatings due to its highest corrosion potential and lowest corrosion current density. When the corrosion occurs, the corrosion rate of coatings S1 and S2 will be higher than that of other coatings due to the higher corrosion current density. In addition, coatings S1 and S2 have more compact microstructure and fine grains, as shown in Fig. 2. Thus, there are more grain boundaries and dislocations, which provide more active nucleation sites for forming continuous and protective passive film rapidly. The passive film plays a key role in preventing Ni ions or electrons from migrating towards the surface to enhance electrochemical reaction and aggravate corrosion. Coatings S1 and S2 contain more Fe because of the higher laser power and twice cladding process, which lead to higher corrosion current density.

3　Conclusions

1) Coatings S1, S2, S3 and S4 can be successfully prepared by laser cladding of Cu-based alloy powder on Q235 steel substrate. Coatings and substrate are strongly bonded. Coatings S1, S2 and S3 have lower diffusion of Fe than coating S4, because the first cladding layer effectively blocks the diffusion of Fe element.

2) Four coatings have the same phases which mainly contain Cu (Ni, Fe) solid solution, Ni(Cr, Mo, Fe) and little intermetallic compounds like $MoNi_4$ and $Mo_{12}Fe_{22}C_{10}$. Cu-enriched phase is in light gray and the other is Fe-enriched phase in dark gray with circle shape.

3) Coatings S1 and S2 with few porosities are produced during the second cladding process which can accelerate the corrosion rate when corrosion occurs.

References

1　Liu Yong. *Advanced Surface Treatment and Testing Techniques for Materials*[M]. Beijing: Science Press, 2008, 155 (in Chinese)

2　Chen Shiqi. *Powder Metallurgy Industry*[J]. 2002(5): 37 (in Chinese)

3　Xia Jin. *Thesis for Master*[D]. Shenyang: Liaoning University, 2016

4　Xu Binshi, Liu Shishan. *Surface Engineering*[M]. Beijing: Machinery Industry Press, 2000: 1 (in Chinese)

5　Khanna A S, Kumari S, Kanungo S *et al*. *International Journal of Refractory Metals and Hard Materials*[J], 2008, 27: 485

6　Sudha C, Shankar P, Subba R V *et al*. *Surface Coating Technology* [J], 2008, 202: 2103

7　Hemmati I, Ocelík V, Hosson J Th M De. *Physics Procedia*[J], 2013, 41: 302

8　Amirreza Farnia, Farshid Malek Ghaini, Jamshid Sabbaghzadeh. *Optics and Lasers in Engineering*[J], 2013, 51(1): 69

9　Xu Peng, Lin Chengxin, Zhou Chaoyu *et al*. *Surface and Coatings Technology*[J], 2014, 238: 9

10　Huang Yongjun. *Optics and Laser Technology*[J], 2010, 43(5): 965

11　Kumar Subrata, Roy Subhransu. *Computational Materials Science*[J], 2007, 41(4): 457.

12　Zhang Xiaofei, Yang Zhongmin, Chen Ying *et al*. *Journal of Iron and Steel Research*[J], 2017(2): 128 (in Chinese)

13　Liu Bing, Liu Lin, Chen Zhenyu. *Acta Metallica Sinica*[J], 2007, 43(1): 82 (in Chinese)

14　Oldfield J W, Masters G W. *CDA Publication*[J], 1996(42): 40

15　Wang Shaohua, Guo Xingwu, Sun Can *et al*. *Transactions of Nonferrous Metals Society of China*[J], 2014, 24: 3810

铜基耐蚀合金熔覆层的制备及耐蚀特性

孔　耀，刘宗德，李　斌

(华北电力大学 电站能量传递转化与系统教育部重点实验室，北京 102206)

摘　要： 采用光纤激光器，在不同功率下在 Q235 钢表面制备了铜基合金熔覆层。利用扫描电镜、能谱仪、X 射线衍射仪和电化学工作站分别对熔覆层的显微结构、相组成及耐蚀性能进行表征。结果表明，熔覆层与基体冶金结合。熔覆层底部为胞状组织，中部为树枝晶和柱状晶。熔覆层主要包含富铜 Cu(Ni, Fe)固溶体和富铁 Ni(Cr, Mo, Fe)固溶体。由于其最高的自腐蚀电位和最低的自腐蚀电流，2000 W 功率下所制备的熔覆层表现出最好的耐蚀性能。

关键词： 铜基合金；激光熔覆；显微结构；耐蚀性能

作者简介：孔　耀，男，1994 年生，博士，华北电力大学电站能量传递转化与系统教育部重点实验室，北京 102206，E-mail：ky@ncepu.edu.cn